

Crystal Structure and Hirshfeld Surface Analysis of Trimethoxy(1-naphthyl)silane – Intermolecular Interactions in a One-Component Single-Crystalline Trimethoxysilane

Jonathan O. Bauer^{*[a]}

Weak intermolecular interactions play a major role in structure formation of molecular crystals. Trimethoxy(1-naphthyl)silane (1), the first one-component single-crystalline trimethoxysilane, was analyzed by single-crystal X-ray diffraction. Weak intermolecular interactions were studied by Hirshfeld surface analysis along with 2D fingerprint plots. Both C(methyl)–H...C and C(naphthyl)–H...C interactions were found. A C(naphthyl)–H...O hydrogen bond between a silicon-bound methoxy oxygen and an aromatic hydrogen atom was identified to be a crucial structure-forming interaction within the crystal packing. Therefore, the tendency of molecular aryl-substituted methoxysilanes to crystallize seems to be mainly dependent on the balance between accessible C–H...O hydrogen bonds and C–H... π interactions.

Introduction

Methoxysilanes are a fundamental class of starting reagents used in preparative chemistry and for the manufacture of a large number of polymers and materials with broad technical applications.^[1] Developing new ways of their synthesis is therefore of great importance.^[2] They are common reagents in sol-gel processes,^[3] used for the protection of hydroxyl groups in organic synthesis,^[4] for surface modifications,^[5] and for the targeted and controlled design of functional silanes^[6] and siloxanes.^[7] Methoxysilanes are also widely used in the Lewis acid-catalyzed Piers-Rubinsztajn coupling of hydrosilanes and alkoxysilanes,^[8] which has proven to be an effective method for the preparation of polysiloxanes.^[9] In recent years, an even greater synthetic potential for methoxysilanes has been discovered when amino functions are incorporated into the molecular framework.^[10] The interplay of amino and methoxy functions

enables highly stereoselective access to asymmetrically substituted silicon centers and provides versatile synthetic building blocks.^[11] In addition, the Si–OMe moiety in aminomethoxysilanes was found to exhibit interesting coordination abilities,^[12] which has led to the development of new chiral ligands.^[11b,13]

Weak intermolecular interactions in molecular crystals have a fundamental structure-forming relevance.^[14] The knowledge which interactions are involved in the aggregation of small molecules in the solid state is therefore of great importance for the understanding of structure-forming processes and for the targeted construction of molecular crystalline frameworks.^[15] In continuation of studies on crystal packing and intermolecular interactions in molecular crystals,^[16] I became interested in a more thorough understanding of the structure-forming principles in molecular, crystalline methoxysilanes. However, given the importance of methoxysilanes, only little information on the solid state structures of methoxysilanes with more than one Si–OMe group is available. Recently, one report was published discussing the crystal packing of single-crystalline dimethoxydimethylsilane after low temperature *in situ* crystallization.^[17] Trimethoxyphenylsilane has already been the subject of research in the context of “ship-in-a-bottle” syntheses.^[18] Although the molecular structure of trimethoxyphenylsilane has previously been investigated as the guest molecule in a single-crystalline host-guest network,^[19] the crystal structure of a one-component trimethoxysilane has not yet been described. In this contribution, I report on the crystal packing and the analysis of intermolecular interactions of the first single-crystalline one-component trimethoxysilane (1).

Results and Discussion

The title compound (1) was synthesized and spectroscopically characterized in a previous work.^[10] Freshly distilled trimethoxy(1-naphthyl)silane (1) crystallized at room temperature in the monoclinic crystal system, space group $P2_1/c$, in the form of colorless blocks, which eventually made a single-crystal X-ray diffraction analysis of a trimethoxysilane possible (Figure 1 and Table 1).

Compound 1 is the first trimethoxysilane obtained in single-crystalline form and examined by X-ray crystallography in its pure form. Since it combines an anisotropic naphthyl and an isotropic Si(OMe)₃ unit, it was of particular interest to subject this compound to a detailed analysis of its crystal packing along with its structure-forming intermolecular interactions. This

[a] Dr. J. O. Bauer
Institut für Anorganische Chemie
Fakultät für Chemie und Pharmazie
Universität Regensburg
Universitätsstraße 31
D-93053 Regensburg, Germany
E-mail: jonathan.bauer@ur.de

© 2021 The Authors. *Zeitschrift für anorganische und allgemeine Chemie* published by Wiley-VCH GmbH. This is an open access article under the terms of the Creative Commons Attribution Non-Commercial NoDerivs License, which permits use and distribution in any medium, provided the original work is properly cited, the use is non-commercial and no modifications or adaptations are made.

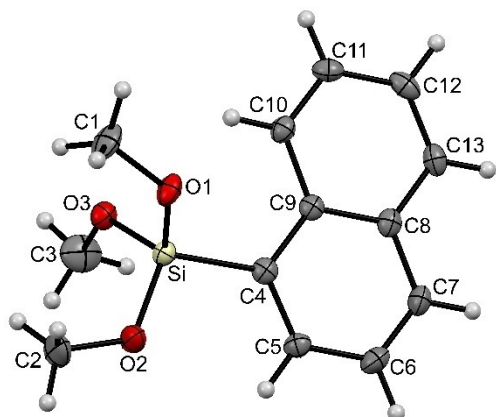


Figure 1. Molecular structure of trimethoxy(1-naphthyl)silane (1) (displacement ellipsoids set at the 50% probability level). Selected bond lengths [Å] and angles [°]: Si–O1 1.6109(12), Si–O2 1.6228(12), Si–O3 1.6228(12), Si–C4 1.8474(17), Si–O1–C1 126.61(12), Si–O2–C2 122.93(12), Si–O3–C3 124.24(13).

Table 1. Crystal data and structure refinement of trimethoxy(1-naphthyl)silane (1).

Empirical formula	C ₁₃ H ₁₆ O ₃ Si
Formula weight [g mol ⁻¹]	248.35
Crystal system	Monoclinic
Space group	P2 ₁ /c
<i>a</i> [Å]	12.7651(8)
<i>b</i> [Å]	7.2298(4)
<i>c</i> [Å]	13.8938(8)
α [°]	90
β [°]	93.513(5)
γ [°]	90
Volume [Å ³]	1279.84(13)
<i>Z</i>	4
Density (calculated) ρ [g cm ⁻³]	1.289
Absorption coefficient μ [mm ⁻¹]	0.177
<i>F</i> (000)	528
Crystal size [mm ³]	0.20 × 0.20 × 0.10
Theta range for data collection θ [°]	2.938–25.998
Index ranges	–15 ≤ <i>h</i> ≤ 15 –8 ≤ <i>k</i> ≤ 8 –17 ≤ <i>l</i> ≤ 17
Reflections collected	15667
Independent reflections	2505 (<i>R</i> _{int} = 0.0362)
Completeness to $\theta = 27.00^\circ$	100.0%
Max. and min. transmission	1.000 and 0.988
Data/restraints/parameters	2505/0/218
Goodness-of-fit on <i>F</i> ²	1.029
Final <i>R</i> indices [<i>I</i> > 2 σ (<i>I</i>)]	<i>R</i> 1 = 0.0341, <i>wR</i> 2 = 0.0904
<i>R</i> indices (all data)	<i>R</i> 1 = 0.0445, <i>wR</i> 2 = 0.0924
Largest diff. peak and hole [e ⁻ ·Å ⁻³]	0.303 and –0.337

model study was performed by means of Hirshfeld surface analysis^[20] in combination with two-dimensional (2D) fingerprint plots^[21] to elucidate basic structural pattern in a single-crystalline trimethoxysilane (Figures 2 and 3). Fingerprint plots provide a two-dimensional view on intermolecular interactions within molecular crystals, which summarizes the three-dimensional picture as captured in the Hirshfeld surface.^[21b] The

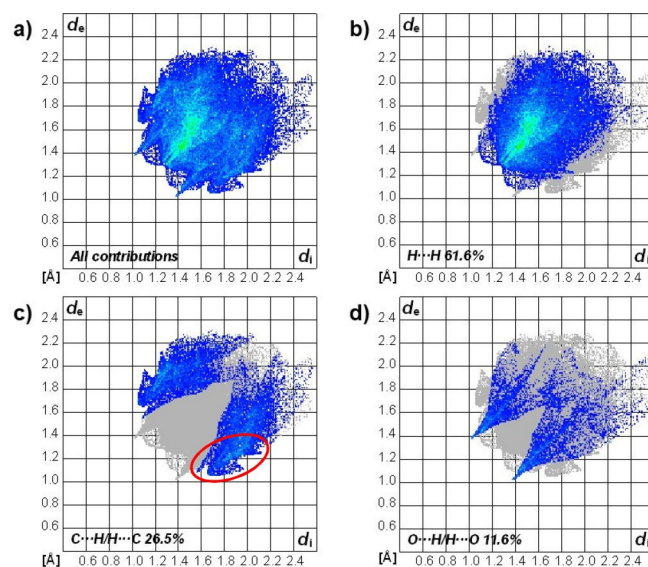


Figure 2. Two-dimensional fingerprint plots for trimethoxy(1-naphthyl)silane (1) showing all contributions of intermolecular contacts (plot a), and resolved in contributions from specific intermolecular pairs of atom types (plots b, c, and d).

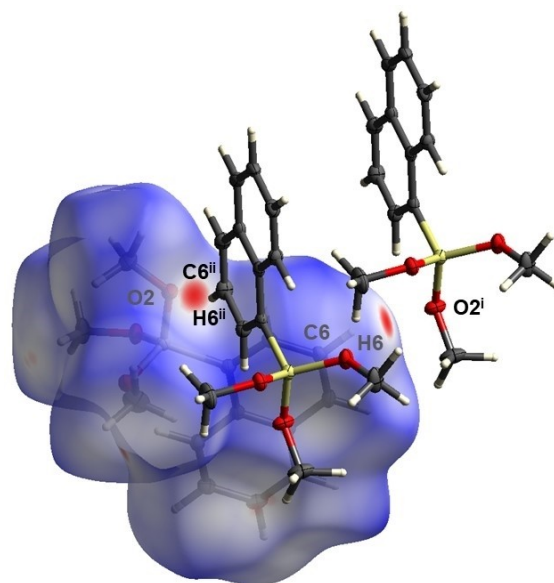


Figure 3. Hirshfeld surface analysis of trimethoxy(1-naphthyl)silane (1) highlighting the weak hydrogen bond between the oxygen atom O2 and the hydrogen atom H6. Bond lengths [Å] and angle [°] of the C6–H6...O2 hydrogen bond: C6–H6 0.965, H6...O2 2.527, C6...O2 3.458, C6–H6...O2 161.88. Symmetry transformations used to generate equivalent atoms: (i) 2–*x*, –0.5 + *y*, 1.5–*z*; (ii) 2–*x*, 0.5 + *y*, 1.5–*z*.

Hirshfeld surface was mapped over d_{norm} ranging from –0.1425 to 1.2480 a.u. d_i and d_e in the 2D fingerprint plots are the distances from the surface to the nearest atom *interior* and *exterior* to the surface, respectively, and are each given in the range of 0.4 to 2.6 Å.^[21]

The fingerprint diagram **a** in Figure 2 shows all contributions of interactions between atoms inside and outside the Hirshfeld surfaces, which can be broken down into the major contributions of individual pairs of atom types to the intermolecular interactions (Figure 2; plots **b**, **c**, and **d**). The dominating intermolecular interactions within the molecular crystal packing can be attributed to H...H contacts (61.6%), followed by C...H/H...C (26.5%), and O...H/H...O (11.6%) contacts. Characteristic features of the 2D fingerprint diagram of trimethoxy(1-naphthyl)silane (**1**) are the rather pronounced blue-green stripe almost along the diagonal and the wings and sharp spikes at the upper left and lower right part of the plot (Figure 2; plot **a**).

Noticeably short H...H contacts^[21a,22] are absent in the crystal structure of compound **1** (Figure 2; plot **b**). The closest H...H contact is approximately 2.6 Å (H10...H12; actually found in the crystal structure: 2.595 Å), i.e. the point on the Hirshfeld surface where $d_i = d_e \approx 1.3$ Å, which is longer than the generally accepted van der Waals radius for hydrogen of 1.2 Å^[23a] and 1.1 Å,^[23b] respectively. The blue-green stripe, where $d_i = d_e$, may be attributed to a considerable number of almost head-to-head H...H contacts^[21a] derived primarily from H...H contacts between silicon-bound methoxy groups.

The characteristic wings (Figure 2; plot **c**) can be ascribed to C—H... π (i.e. H...C) interactions that derive from the anisotropic shape of the naphthyl group. A closer look at the edges of diagram **c** (see red circle) also shows noticeable spikes and, albeit only weakly pronounced, a sawtooth wing shape (a small wing slightly above the larger one) similar to that in the fingerprint diagram for anthracene.^[21] The major wing, which is slightly reminiscent of the wing shape in the fingerprint diagram for naphthalene, most likely corresponds to C—H... π contacts with the C—H bonds pointing more towards the edge of the aromatic ring.^[21] In fact, two types of more edge-shifted C(methyl)—H... π interactions each with one of the two condensed rings of the naphthyl group and on the same side of the ring plane can be identified in the crystal packing. It is known that methyl groups can serve as hydrogen donors in C—H... π interactions and can play a significant role in controlling the crystal structure.^[24] The closest C(methyl)—H...C contact of this type was indeed found to be 2.834 Å (C1—H1A...C12). The only weakly pronounced small wing in the larger area of C—H... π contacts (located at $d_i \approx 2.0$ Å, $d_e \approx 1.3$ Å) might be the result of a more centered C(naphthyl)—H...C interaction that can indeed be identified in the crystal packing between the C11—H11 bond and the π system of the unsubstituted fused ring of the naphthyl group (average H...C distance: 3.343 Å). The spikes visible in the C...H contact diagram **c** are an interesting feature, which reflects the different possible orientations of C—H bonds to the plane of the aromatic ring. This shortest C—H... π contact near 2.7 Å (i.e. $d_i \approx 1.6$ Å, $d_e \approx 1.1$ Å) belongs to a C—H bond that points almost directly to a single atom of the aromatic ring (C10—H10...C12; actually found in the crystal structure: 2.769 Å) and is therefore more reminiscent of the typical fingerprint shapes for hydrogen bonds (compare also with plot **d** in Figure 2).^[21]

The two sharp and distinctive spikes in the fingerprint diagram highlighting C—H...O contacts (Figure 2, plot **d**) are characteristic for the anisotropic nature of hydrogen bonding. The shortest intermolecular distance within the crystal packing of the title compound (**1**) is 2.527 Å and can be assigned to the H...O contact of the C6—H6...O2 hydrogen bond (C6...O2 3.458 Å, C6—H6...O2 161.88°) between the naphthyl and an Si—OMe group, which is highlighted by the red spots on the Hirshfeld surface (Figure 3). The fact that the hydrogen bond acceptor atom (O2) is also part of the smallest Si—O—C bond angle [122.93(12)°] also indicates a significant interaction (Figure 1). The role of C—H...O hydrogen bonds in structural chemistry and biology has often been discussed.^[25] They are generally considered weak according to Jeffrey's classification^[14a,26] with bond energies typically ≤ 2 kcal mol⁻¹, and are composed of a non-directional van der Waals and a directional electrostatic contribution also depending on the polarization of the C—H donor.^[27–29] This leads to a high flexibility of C—H...O hydrogen bonds in terms of distance and geometry.^[27] The distances (C6...O2 and H6...O2) of the C—H...O contact in compound **1** are shorter than the sum of the van der Waals radii.^[23] The C—H...O bond angle of 161.88° is astonishingly close to linearity with the C—H bond pointing in the direction of the oxygen lone electron pairs.^[30] Both findings indicate a noticeable electrostatic component of the hydrogen bond.^[27,31] There is consensus that the distances of a hydrogen bond are not a criterion for the actual strength of the bond, since electrostatic contributions act well beyond the van der Waals distances.^[14b,15,27,28,31]

Conclusions

In conclusion, a thorough model study on intermolecular interactions in a single-crystalline trimethoxysilane (**1**) was carried out by applying the powerful method of Hirshfeld surface analysis along with 2D fingerprint plots. Isotropic H...H van der Waals interactions probably play only a minor role for the crystal structure formation. Instead, it has been shown that the presence of the naphthyl ring enables a variety of different types of more anisotropic intermolecular C—H... π interactions in the crystal structure, i.e. C(methyl)—H...C, longer and closer C(naphthyl)—H...C, and C(naphthyl)—H...O contacts, which form the essential part of attractive structure-forming interactions. The C—H...O hydrogen bond is likely to have a pronounced electrostatic nature with a long range attractive contribution, which can also have an orienting effect during structure formation. It seems crucial to me that 1) the unsubstituted fused ring of the naphthyl group is predominantly involved in all these intermolecular interactions and 2) that the methoxy groups act both as C—H donors in C(methyl)—H... π interactions and as oxygen lone electron pair donors in C—H...O hydrogen bonds. I therefore assume that the tendency of aryl-substituted trimethoxysilanes to crystallize is greater, the easier C—H...O hydrogen bonds are accessible and anisotropic C—H... π interactions can be formed, leading to a well-balanced mix of intermolecular interactions. Not only a successive substitution of methoxy by aryl groups would shift this balance of stabilizing

interactions, but also a change of the anisotropy of the aryl substituent. These findings can explain why, for example, phenyl-,^[10] mesityl-,^[32] cyclohexyl-,^[13b] *tert*-butyltrimethoxysilane,^[10] and aminomethyl-functionalized trimethoxysilanes^[10,33] are liquids at room temperature, and why diphenyl-,^[10] 1-naphthylphenyl-,^[11a] and mesitylphenyldimethoxysilane^[7d] also show no tendency to crystallize at room temperature. On the other hand, methoxytriphenylsilane^[34] forms single-crystals at room temperature, which is associated with an increasing importance of directional C–H $\cdots\pi$ interactions and totally in line with the results described herein. This contribution on structure-relevant interactions can be of interest for the use of methoxysilanes for the design of new functional molecular solids.

Experimental Section

General Remarks: Trimethoxy(1-naphthyl)silane (1) was synthesized according to a published procedure.^[10] Colorless blocks suitable for single-crystal X-ray diffraction analysis were obtained from a freshly distilled sample after slow crystallization at room temperature.

X-Ray Crystallography: Single-crystal X-ray diffraction analysis of trimethoxy(1-naphthyl)silane (1) was performed on an Oxford Diffraction CCD Xcalibur S Diffractometer equipped with a Sapphire3 CCD detector at 173(2) K using graphite-monochromated Mo- $K\alpha$ radiation ($\lambda = 0.71073$ Å). Data collection and reduction was performed using the CrysAlisPro software system, version 1.171.33.55.^[35] The crystal structure was solved with SHELXS-97^[36,37] and a full-matrix least-squares refinement based on F^2 was carried out with SHELXL-2018/3^[37–39] using Olex2^[40] and the SHELX program package as implemented in WinGX.^[41] A multi-scan absorption correction using spherical harmonics as implemented in SCALE3 ABSPACK was employed.^[35] The non-hydrogen atoms were refined using anisotropic displacement parameters. The hydrogen atoms were located on the difference Fourier map and refined independently. Details on crystal data and structure refinement are summarized in Table 1. Figure 1 was created using Mercury 4.1.0.^[42] The Hirshfeld surface and 2D fingerprint plots including Figures 2 and 3 were created using CrystalExplorer 17.5.^[43]

Crystallographic data (excluding structure factors) for the structure in this paper have been deposited with the Cambridge Crystallographic Data Centre, CCDC, 12 Union Road, Cambridge CB21EZ, UK. Copies of the data can be obtained free of charge on quoting the depository number CCDC-2048744 for compound 1 (Fax: +44-1223-336-033; E-Mail: deposit@ccdc.cam.ac.uk; <http://www.ccdc.cam.ac.uk>).

Acknowledgements

The Elite Network of Bavaria (ENB), the Bavarian State Ministry of Science and the Arts (StMWK), and the University of Regensburg are gratefully acknowledged for financial support (N-LW-NW-2016-366). In addition, I thank Prof. Dr. Manfred Scheer and Prof. Dr. Jörg Heilmann for generous and continuous support and excellent working conditions. Open access funding enabled and organized by Projekt DEAL.

Keywords: Hirshfeld surface · Methoxysilanes · Silicon · Structure elucidation · Weak interactions

- [1] a) R. G. Jones, W. Ando, J. Chojnowski (Eds.), *Silicon-Containing Polymers: The Science and Technology of Their Synthesis and Applications*, Springer, Netherlands, **2000**; b) U. Schubert, N. Hüsing, *Synthesis of Inorganic Materials* (4th Ed.), Wiley-VCH, Weinheim, **2019**.
- [2] R. Wakabayashi, Y. Sugiura, T. Shibue, K. Kuroda, *Angew. Chem. Int. Ed.* **2011**, *50*, 10708–10711; *Angew. Chem.* **2011**, *123*, 10896–10899.
- [3] C. J. Brinker, G. W. Scherer, *Sol-Gel Science: The Physics and Chemistry of Sol-Gel Processing*, Academic Press, Inc., San Diego, **1990**.
- [4] P. G. M. Wuts, T. W. Greene, *Greene's Protective Groups in Organic Synthesis* (4th Ed.), John Wiley & Sons, Inc., Hoboken, **2006**.
- [5] a) T. Deschner, Y. Liang, R. Anwender, *J. Phys. Chem. C* **2010**, *114*, 22603–22609; b) N. García, J. Guzmán, E. Benito, A. Esteban-Cubillo, E. Aguilar, J. Santarén, P. Tiemblo, *Langmuir* **2011**, *27*, 3952–3959; c) S. P. Pujari, L. Scheres, A. T. M. Marcellis, H. Zuilhof, *Angew. Chem. Int. Ed.* **2014**, *53*, 6322–6356; *Angew. Chem.* **2014**, *126*, 6438–6474.
- [6] a) R. Tacke, R. Bertermann, C. Burschka, S. Dragota, *Angew. Chem. Int. Ed.* **2005**, *44*, 5292–5295; *Angew. Chem.* **2005**, *117*, 5426–5429; b) J. O. Bauer, J. Stiller, E. Marqués-López, K. Strohfeldt, M. Christmann, C. Strohmman, *Chem. Eur. J.* **2010**, *16*, 12553–12558; c) E. R. Barth, A. Krupp, F. Langenohl, L. Brieger, C. Strohmman, *Chem. Commun.* **2019**, *55*, 6882–6885; d) L. Zibula, M. Achternbosch, J. Wattenberg, F. Otte, C. Strohmman, *Z. Anorg. Allg. Chem.* **2020**, *646*, 978–984; e) T. Lainer, M. Leypold, C. Kugler, R. C. Fischer, M. Haas, *Eur. J. Inorg. Chem.* **2021**, 529–533.
- [7] a) A. Shimojima, K. Kuroda, *Angew. Chem. Int. Ed.* **2003**, *42*, 4057–4060; *Angew. Chem.* **2003**, *115*, 4191–4194; b) R. Wakabayashi, K. Kawahara, K. Kuroda, *Angew. Chem. Int. Ed.* **2010**, *49*, 5273–5277; *Angew. Chem.* **2010**, *122*, 5401–5405; c) M. Yoshikawa, Y. Tamura, R. Wakabayashi, M. Tamai, A. Shimojima, K. Kuroda, *Angew. Chem. Int. Ed.* **2017**, *56*, 13990–13994; *Angew. Chem.* **2017**, *129*, 14178–14182; d) N. A. Espinosa-Jalapa, J. O. Bauer, *Z. Anorg. Allg. Chem.* **2020**, *646*, 828–834.
- [8] a) D. J. Parks, W. E. Piers, *J. Am. Chem. Soc.* **1996**, *118*, 9440–9441; b) S. Rubinsztajn, J. A. Cella, *Macromolecules* **2005**, *38*, 1061–1063.
- [9] a) D. B. Thompson, M. A. Brook, *J. Am. Chem. Soc.* **2008**, *130*, 32–33; b) J. Yu, Y. Liu, *Angew. Chem. Int. Ed.* **2017**, *56*, 8706–8710; *Angew. Chem.* **2017**, *129*, 8832–8836.
- [10] J. O. Bauer, C. Strohmman, *Chem. Commun.* **2012**, *48*, 7212–7214.
- [11] a) J. O. Bauer, C. Strohmman, *Angew. Chem. Int. Ed.* **2014**, *53*, 720–724; *Angew. Chem.* **2014**, *126*, 738–742; b) J. O. Bauer, C. Strohmman, *Eur. J. Inorg. Chem.* **2016**, 2868–2881.
- [12] J. O. Bauer, C. Strohmman, *Organometallics* **2021**, *40*, 11–15.
- [13] a) J. O. Bauer, C. Strohmman, *Angew. Chem. Int. Ed.* **2014**, *53*, 8167–8171; *Angew. Chem.* **2014**, *126*, 8306–8310; b) J. O. Bauer, C. Strohmman, *J. Am. Chem. Soc.* **2015**, *137*, 4304–4307.
- [14] a) T. Steiner, *Angew. Chem. Int. Ed.* **2002**, *41*, 48–76; *Angew. Chem.* **2002**, *114*, 50–80; b) G. R. Desiraju, *Acc. Chem. Res.* **2002**, *35*, 565–573; c) J. L. Atwood, G. W. Gokel, L. J. Barbour (Eds.), *Comprehensive supramolecular chemistry II* (2nd ed.), Elsevier Ltd., Amsterdam, Oxford, Cambridge, **2017**, Vols. 1–9.
- [15] a) G. R. Desiraju, *Angew. Chem. Int. Ed. Engl.* **1995**, *34*, 2311–2327; *Angew. Chem.* **1995**, *107*, 2541–2558; b) G. R. Desiraju, *Angew. Chem. Int. Ed.* **2007**, *46*, 8342–8356; *Angew. Chem.*

- 2007, 119, 8492–8508; c) G. R. Desiraju, *J. Am. Chem. Soc.* **2013**, 135, 9952–9967.
- [16] a) J. O. Bauer, C. Strohmman, *J. Organomet. Chem.* **2015**, 797, 52–56; b) J. O. Bauer, C. Strohmman, *Inorganics* **2017**, 5, 88; c) J. O. Bauer, *Z. Kristallogr. NCS* **2020**, 235, 353–356; d) J. O. Bauer, *Main Group Met. Chem.* **2020**, 43, 1–6.
- [17] I. V. Fedyanin, A. F. Smol'yakov, K. A. Lyssenko, *Mendeleev Commun.* **2019**, 29, 531–533.
- [18] M. Yoshizawa, T. Kusukawa, M. Fujita, K. Yamaguchi, *J. Am. Chem. Soc.* **2000**, 122, 6311–6312.
- [19] K. Biradha, M. Fujita, *J. Inclusion Phenom. Macrocyclic Chem.* **2001**, 49, 201–208.
- [20] a) M. A. Spackman, P. G. Byrom, *Chem. Phys. Lett.* **1997**, 267, 215–220; b) M. A. Spackman, D. Jayatilaka, *CrystEngComm* **2009**, 11, 19–32.
- [21] a) M. A. Spackman, J. J. McKinnon, *CrystEngComm* **2002**, 4, 378–392; b) J. J. McKinnon, D. Jayatilaka, M. A. Spackman, *Chem. Commun.* **2007**, 3814–3816.
- [22] a) J. O. Bauer, C. Strohmman, *Acta Crystallogr. Sect. E* **2010**, 66, o461–o462; b) A. Krupp, E. R. Barth, R. Seymen, C. Strohmman, *Acta Crystallogr. Sect. E* **2020**, 76, 1514–1519.
- [23] a) A. Bondi, *J. Phys. Chem.* **1964**, 68, 441–451; b) For a more accurate determination of the van der Waals radius of hydrogen, see: R. S. Rowland, R. Taylor, *J. Phys. Chem.* **1996**, 100, 7384–7391.
- [24] V. R. Thalladi, R. Boese, S. Brasselet, I. Ledoux, J. Zyss, R. K. R. Jetti, G. R. Desiraju, *Chem. Commun.* **1999**, 1639–1640.
- [25] G. R. Desiraju, T. Steiner, *The Weak Hydrogen Bond in Structural Chemistry and Biology*, Oxford University Press, Oxford, **1999**.
- [26] G. A. Jeffrey, *An Introduction to Hydrogen Bonding*, Oxford University Press, Oxford, **1997**. Hydrogen bonds are designated as weak or strong if their bond energy is below or above the range of 4–15 kcal mol⁻¹ (i.e. the energy range of moderate hydrogen bonds that resemble those between water or carbohydrate molecules); see also ref. 14a.
- [27] T. Steiner, *Chem. Commun.* **1997**, 727–734.
- [28] T. Steiner, G. R. Desiraju, *Chem. Commun.* **1998**, 891–892.
- [29] The C–H donor ability generally depends on the hybridization of the carbon atom: C(sp)–H > C(sp²)–H > C(sp³)–H; see ref. 27 and 28.
- [30] a) A. C. Legon, D. J. Millen, *Acc. Chem. Res.* **1987**, 20, 39–46; b) A. C. Legon, D. J. Millen, *Chem. Soc. Rev.* **1987**, 16, 467–498.
- [31] G. R. Desiraju, *Acc. Chem. Res.* **1991**, 24, 290–296.
- [32] R. Tamaki, S. Han, Y. Chujo, *Silicon Chem.* **2002**, 1, 409–416.
- [33] R. Tacke, J. Sperlich, C. Strohmman, G. Mattern, *Chem. Ber.* **1991**, 124, 1491–1496.
- [34] E. Brendler, T. Heine, W. Seichter, J. Wagler, R. Witter, *Z. Anorg. Allg. Chem.* **2012**, 638, 935–944.
- [35] Oxford Diffraction Ltd., CrysAlisPro Software System, **2010**.
- [36] G. M. Sheldrick, *SHELXS-97*, Universität Göttingen, Göttingen (Germany), **1997**.
- [37] G. M. Sheldrick, *Acta Crystallogr. Sect. A* **2008**, 64, 112–122.
- [38] G. M. Sheldrick, *Acta Crystallogr. Sect. C* **2015**, 71, 3–8.
- [39] G. M. Sheldrick, *SHELXL-2018*, Universität Göttingen, Göttingen (Germany), **2018**.
- [40] O. V. Dolomanov, L. J. Bourhis, R. J. Gildea, J. A. K. Howard, H. Puschmann, *J. Appl. Crystallogr.* **2009**, 42, 339–241.
- [41] L. J. Farrugia, *J. Appl. Crystallogr.* **2012**, 45, 849–854.
- [42] C. F. Macrae, P. R. Edgington, P. McCabe, E. Pidcock, G. P. Shields, R. Taylor, M. Towler, J. van de Streek, *J. Appl. Crystallogr.* **2006**, 39, 453–457.
- [43] M. J. Turner, J. J. McKinnon, S. K. Wolff, D. J. Grimwood, P. R. Spackman, D. Jayatilaka, M. A. Spackman, *CrystalExplorer17*, University of Western Australia, **2017**.

Manuscript received: January 22, 2021

Revised manuscript received: February 16, 2021

Accepted manuscript online: February 17, 2021